Check for updates

Integrated experimental and theoretical insights into CO_2 fixation: tetraazamacrocyclic catalysts in ionic liquids for cyclic carbonate formation†

Jessica Honores, [ID] *[ab] Diego Quezada, [ID] [c] María B. Camarada,[de] Galo Ramirez [ID] [ab] and Mauricio Isaacs [ID] *[ab]

The electrochemical cycloaddition of carbon dioxide to epoxides was investigated using tetraazamacrocyclic metal complexes as electrocatalysts in ionic liquids under mild conditions. The process was carried out in the absence of additional organic solvents, employing $Ni(cyclam)Cl_2$ and $Co(cyclam)Cl_2Cl$ as catalysts, which facilitated the activation of CO_2. The electrosynthesis was conducted in 1-butyl-3-methylimidazolium-based ionic liquids, which not only acted as solvents but also played a crucial role in promoting epoxide ring opening and stabilizing reaction intermediates. Electrochemical experiments using propylene oxide, styrene oxide, and epichlorohydrin demonstrated that the nature of the epoxide substituent significantly impacts the formation of cyclic carbonates. The highest yields were obtained when BMImBr was used as the reaction medium, while other ionic liquids such as $BMImBF_4$ and BMImTFSI resulted in negligible conversion. Spectroelectrochemical studies provided additional insights into the reaction mechanism, confirming the role of halide anions in facilitating carbonate formation. Furthermore, density functional theory (DFT) calculations were performed to explore the interaction between Ni(cyclam) complexes and CO_2. Theoretical results indicate that the *trans*-I isomer of $[Ni(cyclam)]^+$ favors CO_2 coordination and activation, which aligns with the experimental findings. Computational analysis also supported the importance of ionic liquid composition in stabilizing key reaction intermediates. This study highlights the potential of electrocatalytic methodologies for the sustainable conversion of CO_2 into high-value chemicals, contributing to the development of greener and more efficient synthetic strategies.

Sustainability spotlight

The increasing concentration of CO_2 in the atmosphere highlights the need for efficient carbon capture and utilization strategies. Electrochemical approaches offer a sustainable alternative by enabling the direct transformation of CO_2 into value-added products under mild conditions. In this work, we investigate tetraazamacrocyclic complexes as electrocatalysts for the electrosynthesis of cyclic carbonates in ionic liquids, demonstrating enhanced catalytic performance and selectivity. The combination of experimental and theoretical studies provides key mechanistic insights into CO_2 activation and carbonate formation, contributing to the design of more efficient and sustainable electrocatalytic systems. This study aligns with the UN Sustainable Development Goals (SDGs) 7 (Affordable and Clean Energy), 9 (Industry, Innovation, and Infrastructure), and 13 (Climate Action) by advancing energy-efficient CO_2 conversion technologies and promoting greener synthetic methodologies.

[a]Facultad de Química y de Farmacia, Pontificia Universidad Católica de Chile, Av. Vicuña Mackenna 4860, Macul, Santiago, Chile

[b]Millenium Institute on Green Ammonia as Energy Vector, Pontificia Universidad Católica de Chile, Santiago 7820436, Chile

[c]Facultad de Ingeniería, Instituto de Ciencias Aplicadas, Universidad Autónoma de Chile, Del Valle 534, Huechuraba, Santiago, Chile

[d]Cluster of Excellence LivMatS @ FIT – Freiburg Center for Interactive Materials and Bioinspired Technologies, University of Freiburg, Georges-Koehler-Allee 105, 79110 Freiburg, Germany

[e]Inorganic Functional Materials and Nanomaterials, Institute of Inorganic and Analytical Chemistry (IAAC), University of Freiburg, Albertstraße 21, 79104 Freiburg, Germany

† Electronic supplementary information (ESI) available. See DOI: https://doi.org/10.1039/d5su00100e

1 Introduction

The atmospheric concentration of carbon dioxide (CO_2) has risen from pre-industrial levels of ∼280 ppm to over 415 ppm today, driving global climate change, ocean acidification, and ecosystem disruption.[1–3] Addressing these challenges demands not only drastic emission cuts but also innovative approaches to capture, store, and valorize CO_2 in the form of value-added chemicals.

Electrochemical CO_2 fixation has emerged as a promising route because it can directly couple renewable electricity to chemical synthesis under mild conditions, minimizing thermal

inputs and aligning with the tenets of green chemistry.[4–9] By modulating the applied potential, one can selectively activate CO_2 toward diverse products without resorting to harsh reagents or extreme pressures.

Among the many CO_2 conversion pathways, the cycloaddition of CO_2 to epoxides to yield cyclic carbonates is particularly attractive. Cyclic carbonates serve as high-performance aprotic solvents, electrolytes in lithium-ion batteries, monomers for polycarbonate production, and fine-chemical intermediates in pharmaceutical syntheses.[10–15] Their broad industrial utility underscores the importance of developing sustainable, scalable methods for their manufacture.

Traditional syntheses of cyclic carbonates often rely on phosgene or its equivalents (di- or polyols) under elevated temperatures and pressures, raising safety and environmental concerns.[16–19] Photocatalytic systems—such as cobalt–phthalocyanine/TiO_2 hybrids—have demonstrated near-quantitative yields under UV or visible irradiation,[20] yet require specialized catalysts and light sources that can limit practicality.

Electrochemical approaches using simple salts (e.g. alkali halides, quaternary ammonium salts) or non-macrocyclic transition-metal complexes have shown proof-of-concept for CO_2–epoxide cycloaddition, but often suffer from low selectivity, long reaction times (>10 h), and the need for large overpotentials (>−2.4 V vs. Ag/AgCl).[16–26] Superbase-based deep eutectic solvents have improved yields at moderate temperatures but still fall short of fully ambient operation.[27]

Ionic liquids (ILs) offer a "green" reaction medium with negligible vapor pressure, wide electrochemical windows, and tunable solvation of charged intermediates. ILs such as BMImBr, BMImBF$_4$, and BMImTFSI have repeatedly been shown to stabilize metal-alkoxide species and facilitate epoxide ring opening, dramatically enhancing cyclic-carbonate formation under mild potentials.[18,28–38] In particular, halide-rich ILs (e.g. BMImBr) excel: the Br^- anion both nucleophilically opens the epoxide and stabilizes ensuing intermediates, leading to higher yields than fluorinated or sulfonyl ILs.[39,40]

Despite these advances, two key gaps remain. First, most electrocatalytic systems to date employ non-macrocyclic catalysts, leaving the influence of well-defined ligand architectures on CO_2 activation largely unexplored. Second, while individual reaction steps have been probed spectroelectrochemically or theoretically, a fully integrated experimental–computational mechanism under truly ambient temperature and pressure is still lacking.

Herein, we introduce tetraazamacrocyclic complexes—Ni(cyclam)Cl$_2$ and Co(cyclam)Cl$_2$Cl—as robust electrocatalysts for CO_2 cycloaddition to epoxides in BMImBr. We combine cyclic voltammetry, controlled-potential electrolysis, FT-IR spectroelectrochemistry, and density-functional-theory (DFT) calculations to dissect the roles of metal isomerism, IL composition, applied potential, and substrate structure in driving high yields of propylene carbonate, styrene carbonate, and epichlorohydrin carbonate.[41]

Our integrated approach not only achieves quantitative conversion (100%) of propylene oxide at −1.8 V vs. Ag/AgCl and ambient conditions but also delivers a unified mechanistic

framework for CO_2 activation in macrocyclic metal complexes. These insights furnish design principles for next-generation electrocatalysts and IL media, advancing sustainable CO_2 utilization in green chemistry and industrial processes.

2 Materials and methods

2.1 Materials

All reagents and solvents used were of analytical grade or higher. The macrocyclic complexes [Ni(cyclam)Cl$_2$] and [Co(cyclam)Cl$_2$]Cl were synthesized following previously reported procedures.[42,43] Elemental analysis confirmed that, for [Ni(cyclam)Cl$_2$], the found percentages were 36.84% C, 7.25% H, and 17.1% N (predicted: 36.4% C, 7.28% H, 17.0% N); for [Co(cyclam)Cl$_3$]Cl, the found values were 34.12% C, 6.91% H, and 15.1% N (predicted: 32.84% C, 6.63% H, 15.33% N). Propylene oxide, styrene oxide, and epichlorohydrin were purchased from Sigma-Aldrich and used without further purification. Carbon dioxide (extra pure, 99.99%) was obtained from INDURA, Chile. The ionic liquids BMImBF$_4$ (1-butyl-3-methylimidazolium tetrafluoroborate), BMImTFSI (1-butyl-3-methylimidazolium bis(trifluoromethylsulfonyl)imide, >98.5%), and BMImBr (1-butyl-3-methylimidazolium bromide) were also purchased from Sigma-Aldrich. Prior to use, all ionic liquids were dried under vacuum at 80 °C for 24 hours, and their water content was verified using a Karl Fisher titrator (all were below 1% w/w). Solvents were handled under air-free conditions using syringes and cannulas.[44]

2.2 Cyclic carbonate preparation

The electrosynthesis of cyclic carbonates was performed in a one-compartment (undivided) cell using a three-electrode configuration. All electrolysis experiments were carried out at 25 °C and atmospheric pressure. A glassy carbon plate (SPI West Chester, PA, USA; geometric area: 3.25 cm^2) was used as the working electrode, a platinum wire served as the counter electrode, and an Ag/AgCl (saturated) electrode specially conditioned for non-aqueous media was employed as the reference electrode.[45] Initially, a solution containing 78 mmol of the ionic liquid and the appropriate catalyst (macrocyclic complex) was prepared and sonicated for uniform mixing. Next, the solution was transferred into the electrochemical cell, and 10 mmol of the chosen epoxide was added. The mixture was stirred for 15 minutes before inserting the electrodes. Two glass tubes were then introduced into the cell: one immersed in the solution near the working electrode to allow the continuous introduction of carbon dioxide, and a second positioned approximately 4 cm above the solution to serve as an exhaust for pressure equilibration. Carbon dioxide was bubbled continuously during the electrolysis (conducted over 8 to 24 hours) while a constant potential of either −1.4 V or −1.8 V (vs. Ag/AgCl) was applied under constant stirring. After electrolysis, the reaction mixture was extracted with diethyl ether and concentrated by rotary evaporation. The resulting colorless liquid was collected and analyzed by ^1H NMR spectroscopy.

2.3 Spectroelectrochemical techniques

FT-IR spectroelectrochemical experiments were carried out using a PTFE spectroelectrochemical cell equipped with a ZnSe ATR crystal on a Pike Veemax III system. In a typical experiment, a solution containing 10 mmol of propylene oxide and 0.8 mmol of $Ni(cyclam)Cl_2$ in 80 mmol of BMImBr was electrolyzed at -1.8 V (vs. Ag/AgCl). Spectra were recorded at 0, 30, 90, and 240 seconds to monitor changes in vibrational bands corresponding to epoxide ring deformation and cyclic carbonate formation.

2.4 Instrumentation

Water titrations were performed using a CRISON Titromatic KF 2S-2B. ^1H NMR spectra were recorded on a BRUKER AVANCE III HD 400 MHz spectrometer. FT-IR measurements were conducted on a Thermo Nicolet iS10 instrument. Routine electrochemical measurements were performed using a CH Instruments 760C potentiostat, while controlled potential electrolysis was carried out with a BASi PWR-3 potentiostat.

3 Theoretical analysis

Theoretical calculations were performed to explore the geometry of $[Ni(cyclam)]^+$ and its interaction with CO_2, as no crystallographic structure is available. $[Ni(cyclam)]^+$ and $[Ni(cyclam)(CO_2)]^+$ were fully optimized at the density functional theory (DFT) level using the Gaussian16 computational package,[46] implementing the Becke's three parameters nonlocal hybrid exchange potential with the nonlocal correlation functional of Lee, Yang, and Parr (B3LYP)[47–49] without any symmetry restriction. The Gaussian-type orbitals, 6–311G(d,p), were used for light atoms,[50] while the Stuttgart-Dresden effective core potential[51] was implemented for transition metal elements. A tight SCF convergence criteria (10^{-8} a. u.) was set in all calculations with the Grimme dispersion correction (D3).[52] Harmonic vibrational frequencies were calculated to ensure that the optimized geometries were minima on the potential energy surface. The PCM solvation model[53] was implemented to simulate an implicit solvent (water) with a dielectric constant $\varepsilon = 78.3553$. The CO_2 binding energy (E_{bind}) was defined according to the following expression: $E_{bind} = E_{[Ni(cyclam) - (CO2)]^+} - (E_{[Ni(cyclam)]^+} + E_{[CO2]})$, which represents the energy difference between the complex and the optimized energies of the free CO_2 molecule and $[Ni(cyclam)]^+$. In addition, based on the experimental results, the structure of the cyclic carbonate propylene with the ionic liquid BMImBr was optimized to identify the zones more prone to react with the activated CO_2.

4 Results and discussion

4.1 Experimental results

To elucidate the electrocatalytic performance of the tetraaza-macrocyclic complexes, a series of experiments were conducted using cyclic voltammetry, controlled potential electrolysis, and spectroelectrochemical techniques. These investigations examined the influence of ionic liquid composition, applied potential, and substrate structure on the formation of cyclic

carbonates from CO_2 and epoxides. The following section details the key experimental findings, which form the basis for a comprehensive mechanistic interpretation. All experiments reported herein were conducted at constant room temperature (25 °C) and atmospheric pressure.

4.1.1 Electrochemical behavior. To investigate the electrocatalytic properties of cyclam-type macrocyclic nickel complexes in the formation of cyclic carbonates, preliminary cyclic voltammetry experiments were conducted in an ionic liquid medium containing epoxide and $Ni(cyclam)Cl_2$. Fig. 1 illustrates the electrochemical behavior of the nickel complex in 1-butyl-3-methylimidazolium tetrafluoroborate ($BMImBF_4$), which functions both as the solvent and supporting electrolyte. The voltammogram of the neat ionic liquid reveals no significant electrochemical activity, confirming the absence of redox-active impurities and validating the electrochemical window used.

In contrast, the cyclic voltammogram of the nickel complex (depicted in red) shows two well-defined redox processes with half-wave potentials ($E_{1/2}$) at 0.42 V and -1.40 V. These correspond to the Ni(II)/Ni(III) and Ni(II)/Ni(I) redox couples, respectively.[54] These results confirm the electrochemical accessibility of both oxidation and reduction states of the nickel center in this macrocyclic environment.

Upon the addition of propylene oxide to the solution containing $Ni(cyclam)Cl_2$, the cyclic voltammogram (shown in green) remains similar in overall profile to that of the nickel complex alone. The redox couple around 0.47 V is only slightly
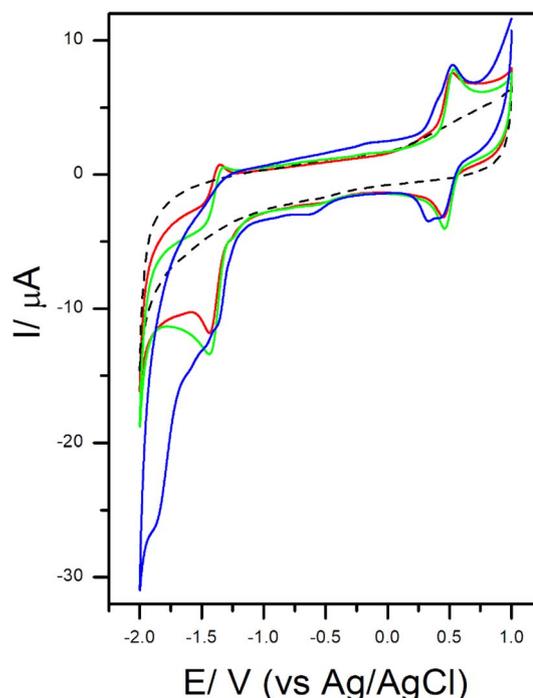

Fig. 1 Electrochemical behavior of $BMImBF_4$ used as solvent (dashed black line), a solution containing 9 mM of $Ni(cyclam)Cl_2$ and $N_{2(sat)}$ (red), addition of propylene oxide (10 mM) saturated with N_2 (green) and saturated with CO_2 (blue). Scan rate: 100 mV s^{-1}, WE: glassy carbon, CE: Pt coil and RE: Ag/AgCl$_{(sat)}$.

shifted and displays a modest increase in current ($\sim$1 μA), while the redox process at -1.4 V becomes more irreversible. Specifically, the anodic current decreases, and the cathodic current increases, suggesting a potential interaction between the reduced form of the complex and the epoxide. The broadening of this signal further supports the presence of such an interaction.

The effect of introducing carbon dioxide to the system is illustrated by the voltammogram shown in blue. At positive potentials, a shoulder emerges in both the anodic and cathodic waves, while at negative potentials, the previously reversible Ni(ii)/Ni(i) redox couple is replaced by an irreversible process, peaking around -1.8 V. This transformation in electrochemical behavior indicates a significant interaction between the nickel complex and CO_2 under reductive conditions.

Taken together, these observations suggest that the irreversible signal observed in the presence of CO_2 likely corresponds to a catalytic reaction involving the activated CO_2 species and the epoxide, mediated by the reduced form of the nickel cyclam complex. These findings highlight the potential of such macrocyclic systems for facilitating electrochemical transformations relevant to carbon capture and conversion in ionic liquid media.

4.1.2 Electrocatalytic synthesis of cyclic carbonates. To evaluate the electrocatalytic activity of the complexes in the electrochemical activation of carbon dioxide and the subsequent electrosynthesis of cyclic carbonates, controlled potential electrolysis was performed under the previously studied conditions.

For these experiments, 78 mmol of ionic liquid (15 mL) and 10 mmol of epoxide were used to obtain the corresponding carbonate, with the catalyst representing 1% of the epoxide concentration. Styrene oxide is less reactive than aliphatic epoxides due to resonance stabilization of its benzylic alkoxide intermediate, which both raises the barrier to ring opening and enables rearrangement pathways that yield benzaldehyde as a detectable by-product under our electrolysis conditions.

Table 1 presents the different parameters varied in each experiment, including time and applied potential varied in each experiment. Additionally, relevant data such as charge and yield are provided.

A comparison of the yield values in experiments I and II indicates that no product is formed in the absence of the metal

complex. This indicates that $BMImBF_4$ under the studied conditions, does not exhibit catalytic activity for this type of reaction.

Electrolysis performed using the $[Ni(cyclam)Cl_2]$ complex as an electrocatalyst, applying the previously established CO_2 reduction potential (-1.4 V) resulted in no conversion to the desired product. Although CO_2 is activated for cycloaddition with the epoxide, the abundance of cations and anions in the reaction medium is insufficient to stabilize the epoxy ring opening. As a result, the cycloaddition reaction remains incomplete.

To assess whether the previously observed negative results are due to slow reaction kinetics, the effect of electrolysis time on conversion yield was investigated. As the reaction time increased from 8 to 24 hours, no detectable conversion to cyclic carbonate was observed in $BMImBF_4$, while only trace amounts (0.33%) were detected in BMImTFSI. This comparison suggests that the absence of product is more likely related to the thermodynamic constraints of the reaction rather than a kinetic limitation.

Experiment VII was conducted by increasing the applied electrochemical potential during the electrolysis to -1.8 V to enhance carbon dioxide activation and promote its subsequent cycloaddition with the epoxide. However, the results remained negative, with 0% conversion observed.

It is important to highlight that the proposed mechanism for this type of reaction[39] relies on the formation of an alkoxide intermediate through epoxide ring opening. The role of the ionic liquid as a stabilizer of the alkoxide species has been identified as a crucial step in the process. Previous reports[39] suggest that the anion of the ionic liquid plays a more significant role than cation, with halides (e.g. Br$-$) demonstrating superior performance compared to fluorinated anions (BF_4^-).

A key finding was obtained in experiment VIII, where a conversion of 59.3% was achieved, confirming that the nature of the anion is critical for the successful electrosynthesis of cyclic carbonate from epoxides. This observation is in strong agreement with previously reported data.

Although our work focused on Br$^-$, Gallardo-Fuentes *et al.* report that in BMImBr the CO_2-propylene oxide cycloaddition yield reaches 72.8%, *versus* 41.1% in $BMImBF_4$ and 26.1% in BMImTFSI.[39] These trends correlate with the conjugate-acid pK_a values (HBr $\approx$ -8, HBF_4 $\approx$ -0.4, HTFSI $\approx$ 1.7), indicating that

Table 1 Optimization of reaction parameters in the electrosynthesis of styrene carbonate from styrene oxide and CO_2 in ionic liquids[a]

Exp.	Ionic liquid	Catalyst	Time (h)	Potential (volts)	Charge (coulomb)	F/mol	Yield %
I	$BMImBF_4$	—	6	-1.4	22	2.3×10^{-2}	0
II	BMImTFSI	—	6	-1.4	18	1.8×10^{-2}	0
III	$BMImBF_4$	$Ni(cyclam)Cl_2$	8	-1.4	33	3.5×10^{-2}	0
IV	BMImTFSI	$Ni(cyclam)Cl_2$	8	-1.4	29	3.0×10^{-2}	0
V	$BMImBF_4$	$Ni(cyclam)Cl_2$	24	-1.4	108	1.1×10^{-1}	0
VI	BMImTFSI	$Ni(cyclam)Cl_2$	24	-1.4	110	1.1×10^{-1}	0.33
VII	$BMImBF_4$	$Ni(cyclam)Cl_2$	24	-1.8	105	1.1×10^{-1}	0
VIII	BMImBr	$Ni(cyclam)Cl_2$	24	-1.8	171	1.77×10^{-1}	59.3

[a] Reaction conditions: 1% cat mol., 78 mmol ionic liquid, 10 mmol styrene oxide.

a more basic, nucleophilic anion promotes the key epoxide-opening step. By analogy, one would expect Cl^- or I^- to follow a similar pattern—driven by their respective acidities—though Br^- offers the optimal balance of ring-opening ability and intermediate stabilization under our conditions.

To investigate the effect of epoxide structure on the electrosynthesis of cyclic carbonates, two additional epoxides-epichlorohydrin and propylene oxide- were used as starting materials. The results obtained from the series of three epoxides in the electrosynthesis of cyclic carbonates are presented below.

Table 2 presents the results of the controlled potential electrolysis (-1.8 V) of the different epoxides, the metal complex and carbon dioxide over a 24-hour period. In general, the results for the epoxide conversion are favorable in all cases, with conversion yields ranging from 17.7% to 100%. It is important to note that the conversion values reported correspond exclusively to the formation of cyclic carbonates, as indicated in the caption of Table 2. Although benzaldehyde was identified as a detectable by-product in reactions involving styrene oxide, it was not quantified in this study. Therefore, the reported data reflect selective product yields rather than total epoxide consumption.

In the cases of electrolysis performed without the addition of a catalyst (Experiments 1, 4, and 7), propylene oxide and epichlorohydrin achieve yields higher than 90%, while styrene oxide reached only 17.7%. The lower reactivity of styrene oxide can be attributed to the stabilization of the benzyl alkoxide intermediate through resonance delocalization (Fig. 2). This effect reduces the nucleophilicity of the alkoxide oxygen, making it less reactive toward the cycloaddition of carbon dioxide, which explains the significantly lower yield observed compared to the other epoxides.

The results obtained for propylene oxide vary considerably in terms of the amount of charge developed. When $Ni(cyclam)Cl_2$ (Experiment 1) complex is used, charge increases almost threefold from the blank (Experiment 1) and conversion rate increases from 93% to 100%. Considering the increase in charge and the slight increase in conversion rate; the reaction time could be too long in Experiment 2 and probably a complete
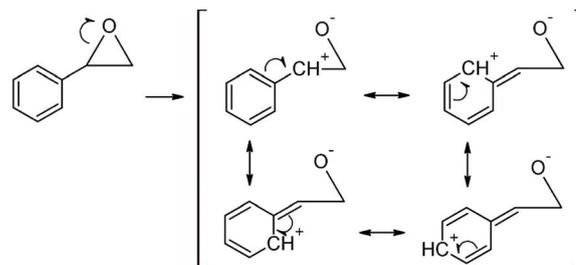

Fig. 2 Resonance stabilization of the alkoxide generated in styrene oxide ring opening.

conversion could be achieved at shorter times, which would further reinforce the idea that the nickel complex studied could be used as a catalyst for the cycloaddition of carbon dioxide to propylene oxide.

A further analysis of Experiment 2 and 3 shows that charge decreases from 290 to 198C when $Ni(cyclam)Cl_2$ is replaced with $[Co(cyclam)Cl_2]Cl$. As expected, the yield in Experiment 2 is slightly higher than Experiment 3, being in good concordance with a higher charge.

Epichlorohydrin electrolysis shows, in all three systems (Experiment 4, 5 and 6), conversions higher than 85%, reaching 99.2% in Experiment 6. Considering the electrocatalytic activity of the cobalt complex against the reduction of carbon dioxide and the intrinsic activity of the ionic liquid, the yield increase shown by $Co(cyclam)^{+3}$ could be related to its ability to stabilize the alkoxide intermediary, rather than by the ability to activate carbon dioxide for its subsequent addition to epichlorohydrin.

Electrolysis carried out with styrene oxide shows significantly lower yields than the other two epoxides, being 17.7% when a catalyst is not used (Experiment 7) and 22.4% when the

Table 2 Conversion to cyclic carbonates in BMImBr at 24 hours of electrolysis at -1.8 V[a]

Exp.	Complex	Epoxide	Charge/C	F/mol	%Conversion
1	—	1	91	0.094	93.0%
2	$Ni(cyclam)Cl_2$		290	0.30	100%
3	$[Co(cyclam)Cl_2]Cl$		198	0.20	98.2%
4	—	2	90	0.093	90.7%
5	$Ni(cyclam)Cl_2$		114	0.12	83.0%
6	$[Co(cyclam)Cl_2]Cl$		176	0.18	99.2%
7	—	3	92	0.095	17.7%
8	$Ni(cyclam)Cl_2$		171	0.18	59.3%
9	$[Co(cyclam)Cl_2]Cl$		103	0.11	22.4%

[a] Reaction conditions: 1% cat. mol., 78 mmol ionic liquid, 10 mmol epoxide at 24 h of electrolysis at -1.8V $vs.$ Ag/AgCl$_{(sat)}$. Epoxide 1: propylene oxide, 2: epichlorohydrin, 3: styrene oxide.
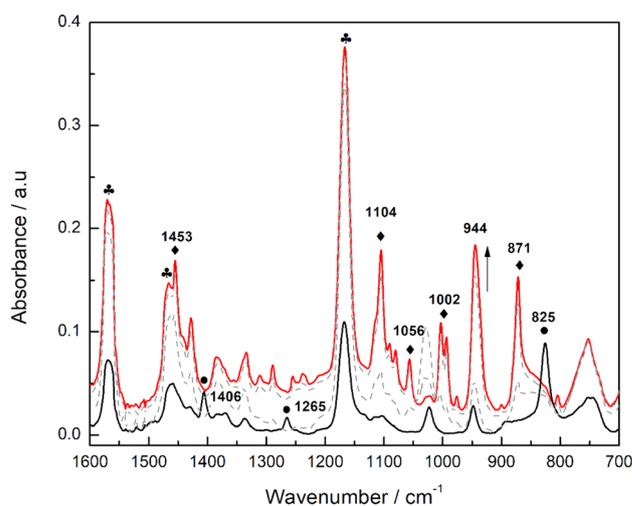

Fig. 3 FTIR/ATR Spectroelectrochemical measurements carried out using a propylene oxide (10 mmol) and $Ni(cyclam)Cl_2$ (0.8 mmol) in BMImBr (80 mmol) solution. Spectra of the solution saturated with CO_2 were taken at 0 seconds (black line), 30 and 90 seconds (dashed line) and at 240 seconds (blue line). Electrolysis was carried out at -1.8V $vs.$ Ag/AgCl. WE: glassy carbon, CE: Pt coil, RE: Ag/AgCl$_{(sat)}$.

cobalt complex is used (Experiment 9). The most interesting result is obtained with the nickel catalyst, in which conversion increases to about 60%. It is also found that the oxide readily reacts with carbon dioxide, forming benzene acetaldehyde (see ESI†), whereby the low yield obtained by electrolysis without catalyst and with the cobalt complex could be explained by the generation of the previously mentioned by-products. On the other hand, the higher yield obtained with nickel catalyst suggests that it could have a higher specificity towards carbonate formation.[25,55]

4.1.3 Spectroelectrochemical analysis. FT-IR spectroelectrochemical measurements were carried out in order to observe spectroscopic evidence that could shed light about the reaction mechanism. A as a model, propylene oxide and $Ni(cyclam)Cl_2$ in a CO_2/BMImBr saturated solution was electrolyzed during 240 seconds at $-1.8V$ *vs.* Ag/AgCl.

Fig. 3 shows the FTIR/ATR spectra of the different species in solution during the electrosynthesis of propylene carbonate. A fast analysis of the spectra shows an evident increase in the bands at 1570, 1167 and 1466 cm^{-1} (♣), all of them appear as the most important changes in the spectra, and are associated to the solvent structure, particularly to deformation of the imidazolium ring.[56,57] Increase in absorbance over time is related to polarization of the electrodes due to lack of convection in the spectroelectrochemical cell. Prior to application of -1.8 V *vs.* Ag/AgCl (black line) propylene oxide spectrum can be observed, showing characteristics bands at 825, 1265 and 1406 cm^{-1}, corresponding to epoxide ring deformation,[58] a band at 944 cm^{-1} can also be observed, related to $-CH_3$ rocking.[59]

When the electrosynthesis starts, a series of changes can be observed all along the spectra. A first group of bands, associated to epoxide ring deformation (●), reduces its absorbance as time passes. As a result, bands are not observed in the last spectrum recorded, meaning that as the reaction takes place, the epoxide ring opens up, forming an alkoxide. A second group of bands can also be detected as the reaction takes place (◆), these signals can be assigned to the cyclic carbonate structure and are mainly associated to vibration modes of the cycle formed between the alkoxide and the activated carbon dioxide. A summary of the most significant FTIR bands can be found in Table 3.

4.2 Theoretical results

In parallel with the experimental studies, density functional theory (DFT) calculations were performed to probe the molecular interactions between the $[Ni(cyclam)]^+$ complex and CO_2. This computational work includes the optimization of *trans*-I and *trans*-III isomers, evaluation of CO_2 binding energies, and analysis of frontier molecular orbitals. These theoretical insights complement the experimental data and provide a deeper understanding of the catalytic process at the molecular level.

Given that the reactivity of $[Ni(cyclam)]^+$ in CO_2 activation is highly dependent on its structural configuration, particular attention was paid to the equilibrium between its *trans*-I and *trans*-III isomers.

$[Ni(cyclam)]^+$ can exist in equilibrium as *trans*-I and *trans*-III isomers. It is reported that in solution, 85% corresponds to the structure *trans*-III.[61] Fig. 4 shows the optimized geometries; according to our computational calculations, *trans*-III is approx. 7.3 kcal mol^{-1} more stable than structure *trans*-I, which has a distorted cycle configuration that influences the planarity of the system. Both structures were subsequently explored for the coordination of CO_2.

Different positions of the CO_2 molecule, considering perpendicular and parallel orientation to the cycle, were built to study the interaction with $[Ni(cyclam)]^+$. In both isomers, the most stable structures corresponded to the parallel alignment. Table 4 summarizes the E_{bind} of the most stable $[Ni(cyclam)(CO_2)]^+$ isomers with some critical bonds and angles.
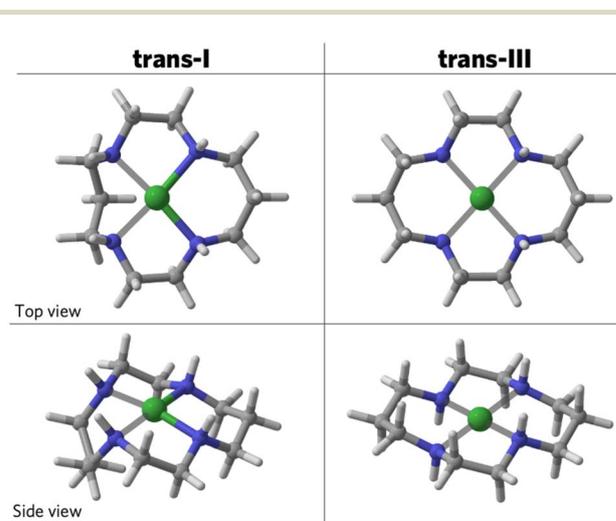

Fig. 4 Optimized geometries of the *trans*-I and *trans*-III isomers of $[Ni(cyclam)]^+$. Color code: carbon atoms are gray, hydrogen in white, nitrogen in blue, and nickel in green.

Table 3 Assignments of the infrared spectra of electrolyzed propylene oxide

cm^{-1}	Description	Ref.	cm^{-1}	Description	Ref.
825	C–O–C ring deformation	58	1167	Imidazole H–C–C & H–C–N bending	56 and 57
871	Symmetric carbonate ring vibration	59	1265	C–O–C ring deformation	58
944	$-O-CO-C-$ symmetric stretching	59	1406	$-O-CH_2$ wagging	59
1002	Alkoxide stretching	60	1453	Imidazole ring C–H stretch	56 and 57
1056	$-C-O-$ ring stretch	59	1466	C–O–C ring deformation	58
1104			1570	Imidazole (ring stretching)	56 and 57

Table 4 Angles and bond lengths of the optimized $[Ni(cyclam)(CO_2)]^+$ structures. The N–Ni distance corresponds to an average of the four lengths

Isomer + CO_2	N–Ni (Å)	N–Ni–N angles (°)		Ni-CO_2 (Å)	E_{bind} (kJ mol^{-1})
trans-I	2.091	84.9	94.2	2.09	−34.873
trans-III	2.099	85.1	94.7	2.13	−29.989

It is important to state that E_{bind} carries an error due to the non-consideration of explicit solvent, counteranions, and entropy. The relative energies between the two isomers are relevant to these calculations.

The most negative value and thus more favorable bonding interaction was detected for the structure *trans*-I (Fig. 5a). This evidence is consistent with the complexes formed with CO that prefer a *trans*-I isomer interaction than *trans*-III.[62] In the case of CO_2, the oxygen atoms are repelled from the amino groups of the cycle, leading to bending in the O–C=O angle in approx. 35° from the planarity. Fig. 5c shows the most stable configuration of $[Ni(cyclam)(CO_2)]^+$ *trans*-III, only 4.88 kJ mol^{-1} less stable than *trans*-I.

In *trans*-I, the carbon atom belonging to the CO_2 molecule is located at 2.09 Å from nickel, and hydrogen bonds also mediate its interaction between the oxygen atoms of carbon dioxide and the amino groups of the cycle with an average distance of 2.48 Å. In the *trans*-III structure, the Ni-C distance is slightly longer (2.13 Å). The HOMO and LUMO frontier orbitals, alpha and beta, were plotted for both systems (Fig. 5b and d). The interaction between CO_2 and the ligand is mainly stabilized through the LUMOs of CO_2 and the β-HOMOs of $[Ni(cyclam)]^+$, primarily the dz^2 of the nickel-metal center. This evidence is in accordance with the work reported recently by Masood and coworkers,[63] who described the $[Ni(cyclam)(CO_2)]^+$ *trans*-III structure at a similar level of theory.

Once the CO_2 is coordinated to $[Ni(cyclam)]^{+,}$ the complex can be attacked by high electronic density centers to produce new molecules like cyclic carbonates. In order to identify these zones, we calculated the dual descriptor of reactivity (DDR) on the *trans*-III structure, which is the most abundant in solution according to experimental reports.[61] The DDR has been defined as a robust indicator of unambiguously nucleophilic and electrophilic sites.[64] DDR is a local reactivity descriptor proposed by Morell and coworkers,[65,66] and is described in terms of the derivative of the Fukui function concerning the number of electrons.[67–69] As shown in Fig. 6a, the DDR plot shows two regions: the yellow zone where nucleophilic attacks can occur, and the red region, where electrophilic reactions can occur. The
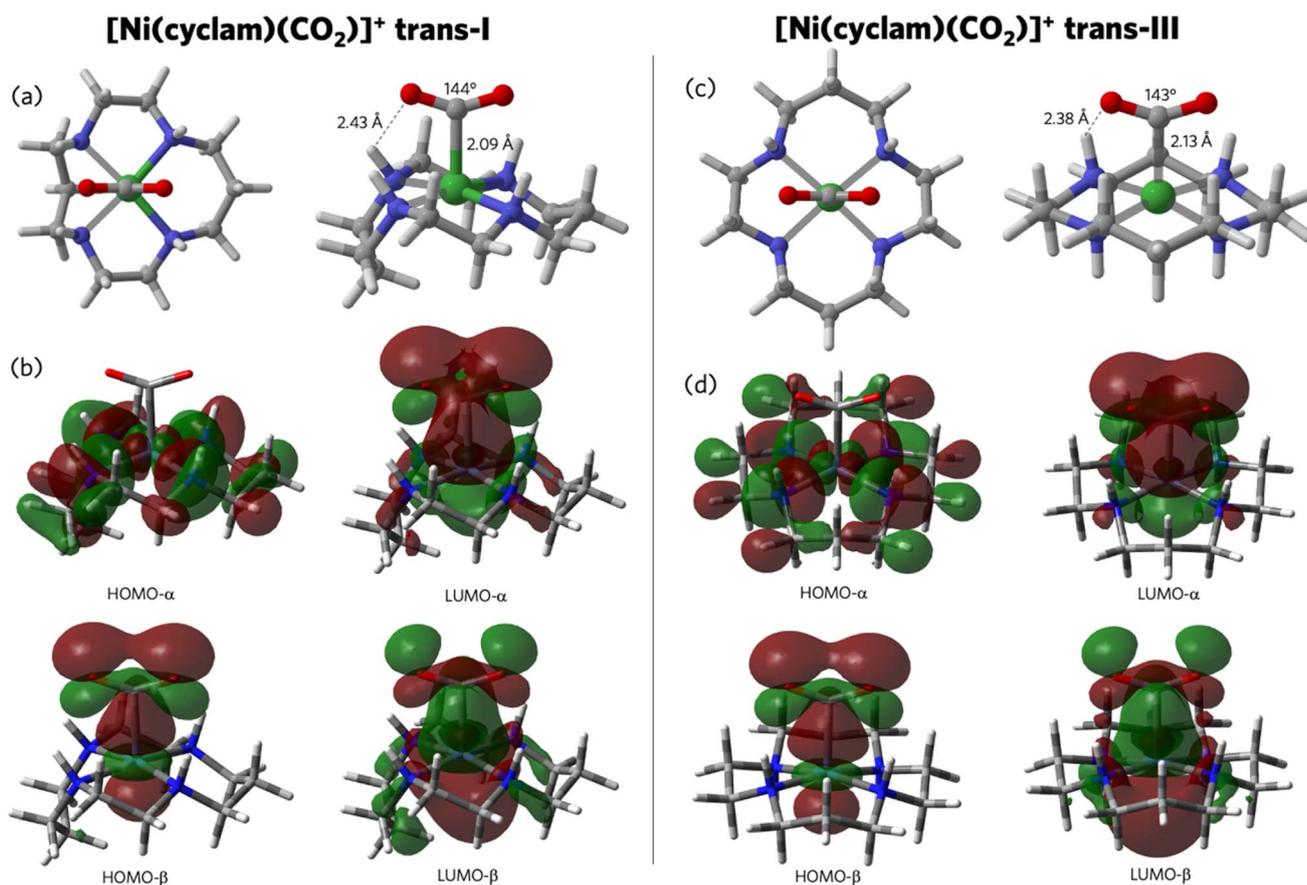

Fig. 5 The optimized structures of $[Ni(cyclam)(CO_2)]^+$ (a) *trans*-I and (c) *trans*-II. (b) and (d) graphical representations of the HOMO and LUMO orbitals of each isomer. Color code: carbon atoms are gray, hydrogen in white, nitrogen in blue, oxygen in red and nickel in green.
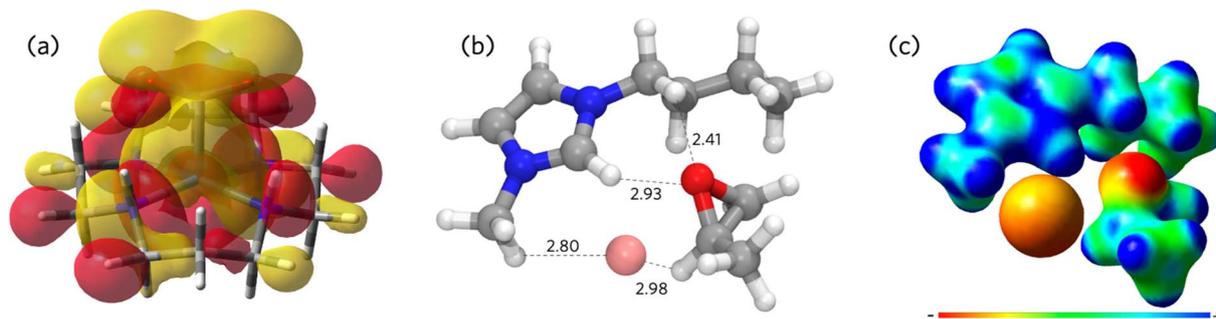
Fig. 6 (a) Dual descriptor of reactivity plot of [Ni(cyclam)(CO$_2$)]$^+$ *trans*-III, (b) the optimized structure of BMImBr and propylene oxide, and its (c) electrostatic potential surface.

carbon atom located at the CO$_2$ has an important density depletion; this electrophilic region can be attacked by a center with high availability of electron density.

According to the experimental evidence, ionic liquids play a key role in opening epoxide rings. The best performance system propylene oxide stabilized by BMImBr ionic liquid was optimized by DFT. Fig. 6b shows the optimized structure and relevant bond distances. The electrostatic potential surface (EPS) was also plotted for this system, reflecting a high-density accumulation in the oxygen atom of the propylene oxide, which can therefore act as a nucleophile and attack the activated carbon atom of the [Ni(cyclam)(CO$_2$)]$^+$ complex, achieving the conversion of epoxide into carbonate.

5 Mechanistic insight

Based on the integrated experimental observations and theoretical calculations, a coherent mechanism for the electrosynthesis of cyclic carbonates is proposed. The DFT results indicate that the [Ni(cyclam)]$^+$ complex exists in a dynamic equilibrium between its *trans*-I and *trans*-III isomers, with the slightly less stable *trans*-I form offering a more favorable site for CO$_2$ coordination. Computed binding energies and reactivity descriptors suggest that once CO$_2$ is activated by the reduced complex, it becomes highly susceptible to nucleophilic attack by the epoxide. In addition, the dual descriptor analysis reveals

distinct electrophilic regions on the coordinated CO$_2$, findings that correlate with the experimental evidence of epoxide ring opening and subsequent cyclic carbonate formation. Collectively, these insights support a mechanism in which the reduced [Ni(cyclam)]$^+$ complex first activates CO$_2$, thereby facilitating nucleophilic attack by the epoxide—an event further promoted by the stabilizing effect of bromide anions—ultimately driving the formation of cyclic carbonates.

Considering the previously discussed evidence and relevant literature reports, a plausible electrosynthesis mechanism for cyclic carbonates is depicted in Fig. 7. In the first step, the carbon dioxide molecule is activated by the reduced metal complex. Subsequently, the activated CO$_2$ reacts with the epoxide, which has been opened by the ionic liquid. The final step involves the addition of another CO$_2$ molecule, leading to ring closure and formation of the desired product. It is worth noting that previous mechanistic studies on metal–salen complexes, particularly those involving Cr(III), have shown that the metal center can coordinate to the oxygen atom of the epoxide ring, thereby increasing the electrophilicity of the adjacent carbon and facilitating nucleophilic attack. This interaction has been proposed as a key step in asymmetric ring-opening reactions catalyzed by such complexes, contributing to both reactivity and selectivity.[70]

6 Conclusion

The electrosynthesis of cyclic carbonates was carried out using cyclam-type metal complexes as electrocatalysts, achieving high conversion yields under optimized conditions. The best performance was obtained using Ni(cyclam)Cl$_2$ in the presence of BMImBr, applying −1.8 V for 24 hours, which highlights the crucial role of the ionic liquid anion in stabilizing key reaction intermediates. In contrast, BMImBF$_4$ and BMImTFSI were ineffective under the same conditions, further supporting the importance of halide-based ionic liquids for promoting the cycloaddition reaction.

The conversion of propylene oxide to propylene carbonate reached 100% when Ni(cyclam)Cl$_2$ was used as a catalyst, demonstrating that electrosynthesis under ambient conditions can provide an efficient alternative to traditional catalytic approaches. The proposed mechanism suggests that CO$_2$
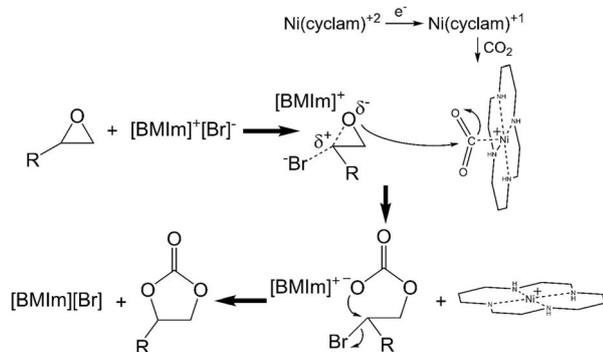

Fig. 7 Mechanism for the electrosynthesis of cyclic carbonates in BMImBr using Ni (cyclam)Cl$_2$ as catalyst in homogeneous medium.

activation occurs through the electrochemical reduction of the metal center, followed by a nucleophilic attack from the epoxide. The presence of Br^- anions in the ionic liquid facilitates the stabilization of the alkoxide intermediate, enabling the formation of the cyclic carbonate.

To further understand the catalytic process, density functional theory (DFT) calculations were performed, providing insight into the electronic structure of [Ni(cyclam)]$^+$ complexes, the binding energy of CO_2, and the differences in reactivity between trans-I and trans-III isomers. The results indicate that CO_2 coordination is more favorable in the trans-I configuration, and that specific electronic properties of the complex play a key role in enhancing reactivity. Additionally, computational analysis of the interaction between the epoxide and the ionic liquid helped to rationalize the experimental observations regarding reaction efficiency and selectivity.

Overall, the combination of electrochemical, spectroelectrochemical, and computational studies provides a comprehensive understanding of the factors influencing the electrocatalytic conversion of CO_2 into cyclic carbonates. These findings contribute to the development of more sustainable methodologies for CO_2 utilization, offering potential applications in green chemistry and industrial processes.

Data availability

The data supporting this article have been included as part of the ESI.†

Conflicts of interest

There are no conflicts of interest to declare.

Acknowledgements

References

1 L.-S. Lau, C.-K. Choong and Y.-K. Eng, Carbon dioxide emission, institutional quality, and economic growth: Empirical evidence in Malaysia, *Renew. Energy*, 2014, **68**, 276–281.

2 A. J. Weaver and C. Hillaire-Marcel, Global Warming and the Next Ice Age, *Science*, 2004, **304**, 400–402.

3 K. Trenberth, A. Dai, G. van der Schrier, P. Jones, J. Barichivich, K. Briffa and J. Sheffield, Global warming and changes in drought, *Nat. Clim. Change*, 2014, **4**, 17–22.

4 J. Inglis, J. Vos, B. MacLean and M. Pryce, Electrocatalytic pathways towards sustainable fuel production from water and CO_2, *Coord. Chem. Rev.*, 2012, **256**, 2571–2600.

5 J. Lee, Y. Kwon, R. Machunda and H. Lee, Electrocatalytic recycling of CO_2 and small organic molecules, *Chem.–Asian J.*, 2009, **4**, 1516–1523.

6 C. F. Leung and P. Y. Ho, Molecular catalysis for utilizing CO_2 in fuel electro-generation and in chemical feedstock, *Catalysts*, 2019, **9**, 760.

7 I. Omae, Recent developments in carbon dioxide utilization for the production of organic chemicals, *Coord. Chem. Rev.*, 2012, **256**(13–14), 1384–1405.

8 E. E. Benson, C. P. Kubiak, A. J. Sathrum and J. M. Smieja, Electrocatalytic and homogeneous approaches to conversion of CO_2 to liquid fuels, *Chem. Soc. Rev.*, 2009, **38**, 89–99.

9 M. K. Leu, I. Vicente, J. A. Fernandes, I. de Pedro, J. Dupont, V. Sans, P. Licence, A. Gual and I. Cano, On the real catalytically active species for CO_2 fixation into cyclic carbonates under near ambient conditions: Dissociation equilibrium of [BMIm][Fe(NO)$_2$Cl$_2$] dependant on reaction temperature, *Appl. Catal., B*, 2019, **245**, 240–250.

10 J. Klankermayer, S. Wesselbaum, K. Beydoun and W. Leitner, Selective Catalytic Synthesis Using the Combination of Carbon Dioxide and Hydrogen: Catalytic Chess at the Interface of Energy and Chemistry, *Angew. Chem., Int. Ed.*, 2016, **55**, 7296–7343.

11 M. Mikkelsen, M. Jørgensen and F. Krebs, The Teraton Challenge. A Review of Fixation and Transformation of Carbon Dioxide, *Energy Environ. Sci.*, 2010, **3**, 43–81.

12 I. Omae, Aspects of carbon dioxide utilization, *Catal. Today*, 2006, **115**, 33–52.

13 M. North, R. Pasquale, C. Young and M. North, Synthesis of cyclic carbonates from epoxides and CO_2, *Green Chem.*, 2010, **12**, 1514–1539.

14 T. Sakakura, J. C. Choi and H. Yasuda, Transformation of carbon dioxide, *Chem. Rev.*, 2007, **107**, 2365–2387.

15 Q.-W. Song, L.-N. He, J.-Q. Wang, H. Yasuda and T. Sakakura, Catalytic fixation of CO_2 to cyclic carbonates by phosphonium chlorides immobilized on fluorous polymer, *Green Chem.*, 2013, **15**, 110–115.

16 V. Calo, A. Nacci, A. Monopoli and A. Fanizzi, Cyclic carbonate formation from carbon dioxide and oxiranes in tetrabutylammonium halides as solvents and catalysts, *Org. Lett.*, 2002, **4**, 2561–2563.

17 W. J. Kruper and D. D. Dellar, Catalytic Formation of Cyclic Carbonates from Epoxides and CO_2 with Chromium Metalloporphyrinates, *J. Org. Chem.*, 1995, **60**, 725–727.

18 H. Yang, Y. Gu, Y. Deng and F. Shi, Electrochemical activation of carbon dioxide in ionic liquid: synthesis of cyclic carbonates at mild reaction conditions, *Chem. Commun.*, 2002, 274–275.

19 R. L. Paddock, Y. Hiyama, J. M. McKay and S. T. Nguyen, Co(III) porphyrin/DMAP: an efficient catalyst system for the synthesis of cyclic carbonates from CO2 and epoxides, *Tetrahedron Lett.*, 2004, **45**, 2023–2026.

20 X. Zhou, Y. Zhang, X. Yang, J. Yao and G. Wang, Hydrated Alkali Metal Halides as Efficient Catalysts for the Synthesis of Cyclic Carbonates from CO_2 and Epoxides, *Chin. J. Catal.*, 2010, **31**, 765–768.

21 M. Wang, Y. She, X. Zhou and H. Ji, Efficient Solvent-free Synthesis of Chloropropene Carbonate from the Coupling Reaction of CO_2 and Epichlorohydrin Catalyzed by Magnesium Porphyrins as Chlorophyll-like Catalysts, *Chin. J. Chem. Eng.*, 2011, **19**, 446–451.

22 D. Bai, X. Wang, Y. Song, B. Li, L. Zhang, P. Yan and H. Jing, Bifunctional Metalloporphyrins-Catalyzed Coupling Reaction of Epoxides and CO_2 to Cyclic Carbonates, *Chin. J. Catal.*, 2010, **31**, 176–180.

23 B. R. Buckley, A. P. Patel and K. G. U. Wijayantha, Electrosynthesis of cyclic carbonates from epoxides and atmospheric pressure carbon dioxide, *Chem. Commun.*, 2011, **47**, 11888.

24 H. Vignesh Babu and K. Muralidharan, Zn(II), Cd(II) and Cu(II) complexes of 2,5-bis{N-(2,6-diisopropylphenyl) iminomethyl}pyrrole: synthesis, structures and their high catalytic activity for efficient cyclic carbonate synthesis, *Dalton Trans.*, 2013, **42**, 1238–1248.

25 J. Honores, D. Quezada, G. Chacón, O. Martínez-Ferraté and M. Isaacs, Synthesis of Cyclic Carbonates from CO_2 and Epoxide Catalyzed by Co, Ni and Cu Complexes in Ionic Liquids, *Catal. Lett.*, 2019, **149**, 1825–1832.

26 L. Schoepff, L. Monnereau, S. Durot, S. Jenni, C. Gourlaouen and V. Heitz, A flexible bis-Co(III) porphyrin cage as a bimetallic catalyst for the conversion of CO_2 and epoxides into cyclic carbonates, *ChemCatChem*, 2020, **12**, 5826–5833.

27 S. García-Argüelles, M. L. Ferrer, M. Iglesias, F. Del Monte and M. C. Gutiérrez, Study of superbase-based deep eutectic solvents as the catalyst in the chemical fixation of CO_2 into cyclic carbonates under mild conditions, *Materials*, 2017, **10**, 759.

28 J. Peng and Y. Deng, Cycloaddition of carbon dioxide to propylene oxide catalyzed by ionic liquids, *New J. Chem.*, 2001, **25**, 639–641.

29 J. Sun, S. Fujita, F. Zhao and M. Arai, Synthesis of styrene carbonate from styrene oxide and carbon dioxide in the presence of zinc bromide and ionic liquid under mild conditions, *Green Chem.*, 2004, **6**, 613.

30 L.-F. Xiao, F.-W. Li, J.-J. Peng and C.-G. Xia, Immobilized ionic liquid/zinc chloride: Heterogeneous catalyst for synthesis of cyclic carbonates from carbon dioxide and epoxides, *J. Mol. Catal. A:Chem.*, 2006, **253**, 265–269.

31 J. Sun, S. Zhang, W. Cheng and J. Ren, Hydroxyl-functionalized ionic liquid: a novel efficient catalyst for chemical fixation of CO_2 to cyclic carbonate, *Tetrahedron Lett.*, 2008, **49**, 3588–3591.

32 E.-H. Lee, J.-Y. Ahn, M. M. Dharman, D.-W. Park, S.-W. Park and I. Kim, Synthesis of cyclic carbonate from vinyl cyclohexene oxide and CO_2 using ionic liquids as catalysts, *Catal. Today*, 2008, **131**, 130–134.

33 D. Yuan, C. Yan, B. Lu, H. Wang, C. Zhong and Q. Cai, Electrochemical activation of carbon dioxide for synthesis of dimethyl carbonate in an ionic liquid, *Electrochim. Acta*, 2009, **54**, 2912–2915.

34 R. A. Sheldon, Green solvents for sustainable organic synthesis: state of the art, *Green Chem.*, 2005, **7**, 267–278.

35 T. Welton, Room-temperature ionic liquids: solvents for synthesis and catalysis, *Chem. Rev.*, 1999, **99**, 2071–2083.

36 H. Tokuda, K. Hayamizu, K. Ishii, A. Bin, H. Susan and M. Watanabe, Physicochemical Properties and Structures of Room Temperature Ionic Liquids 1 Variation of Anionic Species, *J. Phys. Chem. B*, 2004, **108**, 16593–16600.

37 P. Hapiot and C. Lagrost, Electrochemical Reactivity in Room-Temperature Ionic Liquids, *Chem. Rev.*, 2008, **108**, 2238–2264.

38 L. E. Barrosse-Antle, A. M. Bond, R. G. Compton, A. M. O'Mahony, E. I. Rogers and D. S. Silvester, Voltammetry in Room Temperature Ionic Liquids: Comparisons and Contrasts with Conventional Electrochemical Solvents, *Chem. Asian J.*, 2010, **5**, 202–230.

39 S. Gallardo-Fuentes, R. Contreras, M. Isaacs, J. Honores, D. Quezada, E. Landaeta and R. Ormazábal-Toledo, On the mechanism of CO_2 electro-cycloaddition to propylene oxides, *J. CO₂ Util.*, 2016, **16**, 114.

40 X. Zhou, J. Weber and J. Yuan, Poly(ionic liquid)s: Platform for CO_2 capture and catalysis, *Curr. Opin. Green Sustainable Chem.*, 2019, **16**, 39–46.

41 R. Francke, B. Schille and M. Roemelt, Homogeneously Catalyzed Electroreduction of Carbon Dioxide—Methods, Mechanisms, and Catalysts, *Chem. Rev.*, 2018, **118**, 4631–4701.

42 B. Bosnich, C. K. Poon and M. L. Tobe, Complexes of Cobalt(III) with a Cyclic Tetradentate Secondary Amine, *Inorg. Chem.*, 1965, **4**, 1102–1108.

43 B. Bosnich, M. L. Tobe and G. A. Webb, Complexes of Nickel(II)with a Cyclic Tetradentate Secondary Amine, *Inorg. Chem.*, 1965, **4**, 1109–1112.

44 J. Errington, *Advanced Practical Inorganic and Metalorganic Chemistry*, Blackie Academic & Professional, an imprint of Chapman & Hall, Wiltshire, Great Britain, 1997.

45 G. A. East and M. A. del Valle, Easy-to-make Ag/AgCl reference electrode, *J. Chem. Educ.*, 2000, **77**, 97.

46 M. J. Frisch, G. W. Trucks, H. B. Schlegel, G. E. Scuseria, M. A. Robb, J. R. Cheeseman, G. Scalmani, V. Barone, G. A. Petersson, H. Nakatsuji, X. Li, M. Caricato, A. V. Marenich, J. Bloino, B. G. Janesko, R. Gomperts, B. Mennucci, H. P. Hratchian, J. V. Ortiz, A. F. Izmaylov, J. L. Sonnenberg, F. D. Williams, F. Lipparini, F. Egidi, J. Goings, B. Peng, A. Petrone, T. Henderson, D. Ranasinghe, V. G. Zakrzewski, J. Gao, N. Rega, G. Zheng, W. Liang, M. Hada, M. Ehara, K. Toyota, R. Fukuda, J. Hasegawa, M. Ishida, T. Nakajima, Y. Honda, O. Kitao, H. Nakai, T. Vreven, K. Throssell, J. A. Montgomery Jr, J. E. Peralta, F. Ogliaro, M. J. Bearpark, J. J. Heyd, E. N. Brothers, K. N. Kudin, V. N. Staroverov, T. A. Keith, R. Kobayashi, J. Normand, K. Raghavachari, A. P. Rendell, J. C. Burant, S. S. Iyengar, J. Tomasi, M. Cossi, J. M. Millam, M. Klene, C. Adamo, R. Cammi, J. W. Ochterski, R. L. Martin, K. Morokuma,

O. Farkas, J. B. Foresman, D. J. Fox, *Gaussian 16. Gaussian 16*2016.

47 A. D. Becke, Density-functional thermochemistry. III. The role of exact exchange, *J. Chem. Phys.*, 1993, **98**, 5648–5652.

48 C. Lee, W. Yang and R. G. Parr, Development of the Colle-Salvetti correlation-energy formula into a functional of the electron density, *Phys. Rev. B*, 1988, **37**, 785–789.

49 P. J. Stephens, F. J. Devlin, C. F. Chabalowski and M. J. Frisch, Ab Initio Calculation of Vibrational Absorption and Circular Dichroism Spectra Using Density Functional Force Fields, *J. Phys. Chem.*, 1994, **98**, 11623–11627.

50 G. A. Petersson, A. Bennett, T. G. Tensfeldt, M. A. Al-Laham, W. A. Shirley and J. Mantzaris, A complete basis set model chemistry. I. The total energies of closed-shell atoms and hydrides of the first-row elements, *J. Chem. Phys.*, 1988, **89**, 2193–2218.

51 M. Dolg, U. Wedig, H. Stoll and H. Preuss, Energy-adjusted *ab initio* pseudopotentials for the first-row transition elements, *J. Chem. Phys.*, 1987, **86**, 866–872.

52 S. Grimme, J. Antony, S. Ehrlich and H. Krieg, A consistent and accurate *ab initio* parametrization of density functional dispersion correction (DFT-D) for the 94 elements H-Pu, *J. Chem. Phys.*, 2010, **132**, 154104.

53 J. Tomasi, B. Mennucci and E. Cances, The use of continuum solvation models in the context of density functional theory, *J. Mol. Struct.:THEOCHEM*, 1999, **464**, 211–226.

54 J. Honores, D. Quezada, M. García, K. Calfumán, J. P. Muena, M. J. Aguirre, M. C. Arévalo and M. Isaacs, Carbon neutral electrochemical conversion of carbon dioxide mediated by $[M^{n+}$ (cyclam)Cl$_n$] (M = Ni^{2+} and Co^{3+}) on mercury free electrodes and ionic liquids as reaction media, *Green Chem.*, 2017, **19**, 1155–1162.

55 H. Khoshro, H. R. Zare, M. Namazian, A. a. Jafari and A. Gorji, Synthesis of cyclic carbonates through cycloaddition of electrocatalytic activated CO$_2$ to epoxides under mild conditions, *Electrochim. Acta*, 2013, **113**, 263–268.

56 K. Srinivas, A. Kumar and S. Chauhan, Epoxidation of alkenes with hydrogen peroxide catalyzed by iron (III) porphyrins in ionic liquids, *Chem. Commun.*, 2002, 2456–2457.

57 W. Wu, W. Li, B. Han, Z. Zhang, T. Jiang and Z. Liu, A green and effective method to synthesize ionic liquids: supercritical CO$_2$ route, *Green Chem.*, 2005, **7**, 701.

58 C. T. Lynch, K. S. Mazdiyasni, J. S. Smith and W. J. Crawford, Infrared Spectra of Transition Metal Alkoxides, *Anal. Chem.*, 1964, **36**, 2332–2337.

59 G. J. Janz, J. Ambrose, J. W. Coutts and J. R. Downey, Raman spectrum of propylene carbonate, *Spectrochim. Acta, Part A*, 1979, **35**, 175–179.

60 M. C. Tobin, The infrared spectrum of propylene oxide, *Spectrochim. Acta*, 1960, **16**, 1108–1110.

61 P. J. Connolly and E. J. Billo, Hydrogen-1 NMR evidence for the R, S, R, S isomer of the (1,4,8,11-tetraazacyclotetradecane) nickel(II) ion, *Inorg. Chem.*, 1987, **26**, 3224–3226.

62 J. D. Froehlich and C. P. Kubiak, The homogeneous reduction of CO$_2$ by [Ni(cyclam)]+: increased catalytic rates with the addition of a CO scavenger, *J. Am. Chem. Soc.*, 2015, **137**, 3565–3573.

63 Z. Masood and Q. Ge, Electrochemical reduction of CO$_2$ to CO and HCOO$^-$ using metal–cyclam complex catalysts: predicting selectivity and limiting potential from DFT, *Dalton Trans.*, 2021, **50**, 11446–11457.

64 J. I. Martínez-Araya, Why is the dual descriptor a more accurate local reactivity descriptor than Fukui functions?, *J. Math. Chem.*, 2015, **53**, 451–465.

65 C. Morell, A. Grand and A. Toro-Labbé, New dual descriptor for chemical reactivity, *J. Phys. Chem. A*, 2005, **109**, 205–212.

66 C. Morell, A. Grand and A. Toro-Labbé, Theoretical support for using the $\Delta f(r)$ descriptor, *Chem. Phys. Lett.*, 2006, **425**, 342–346.

67 R. G. Parr, *Horizons of Quantum Chemistry*, Springer, Netherlands, Dordrecht, 1980, pp. 5–15.

68 H. Chermette, Chemical reactivity indexes in density functional theory, *J. Comput. Chem.*, 1999, **20**, 129–154.

69 P. Geerlings, F. De Proft and W. Langenaeker, Conceptual Density Functional Theory, *Chem. Rev.*, 2003, **103**, 1793–1874.

70 A. Lidskog, Y. Li and K. Wärnmark, Asymmetric Ring-Opening of Epoxides Catalyzed by Metal–Salen Complexes, *Catalysts*, 2020, **10**, 705.